JTTEES 21:314–324
DOI: 10.1007/s11666-011-9705-2
1059-9630/$19.00 © ASM International

Influence of Surface Finishing on the Oxidation Behaviour of VPS MCrAlY Coatings

Alessio Fossati, Martina DiFerdinando, Ugo Bardi, Andrea Scrivani, and Carlo Giolli

(Submitted July 29, 2011; in revised form October 17, 2011)

CoNiCrAlY coatings were produced by means of the vacuum plasma spraying (VPS) process onto CMSX-4 single crystal nickel superalloy disk substrates. As-sprayed samples were annealed at high temperatures in low vacuum. Three kinds of finishing processes were carried out, producing three types of samples: as-sprayed, mechanically smoothed by grinding, ground and PVD coated by using aluminum targets in an oxygen atmosphere. Samples were tested under isothermal conditions, in air, at 1000 °C, and up to 5000 h. Morphological, microstructural and compositional analyses were performed on the coated samples in order to assess the high temperature oxidation behavior provided by the three different surface finishing processes. Several differences were observed: grinding operations decrease the oxidation resistance, whereas the PVD process can increase the performances over longer time with respect of the as-sprayed samples.

Keywords corrosion protection, high temperature application, MCrAlY, protective coatings

1. Introduction

Thermal barrier coatings (TBCs) consist of a multilayered system formed by an yttria partially-stabilized zirconia (YPSZ) top coat and an MCrAlY (M = Ni, Co, Fe) bond coat. The top coat makes it possible to increase the gas turbine engine operating temperature and to enhance the efficiency without raising the base metal temperature. MCrAlY coatings are commonly used for oxidation protection of high-temperature components of gas turbine, even without the presence of the ceramic top coat, because they can form a protective surface scale during high-temperature service (Ref 1, 2).

The failure of a TBC system usually occurs due to the delamination of the coating layers. Cracks, leading to the delamination of the top coat, can nucleate and propagate inside or next to the thermally grown oxide (TGO) scale that forms at the interface of the top and bond coat (Ref 3–5). The types of oxide that a bond coat can develop are related to the thermodynamic conditions and to the specific chemical composition of the alloy. Depending on the chemical composition of the coating NiO, Cr_2O_3, Al_2O_3, spinel oxides or a mixture of them can grow, due to the selective oxidation of some elements. If the oxide scale is formed by a slow-growing, stable and dense oxide layer, high temperature oxidation resistance and thus a longer lifetime of the TBC can be achieved. It is preferred that this oxide scale be a dense and continuous α-alumina layer (α-Al_2O_3) (Ref 6–8), because this kind of oxide protects the bond coat from further oxidation, owing to its low diffusivity of oxygen and metallic elements (Ref 9). Selective oxidation of Al occurs only on the surface of an alloys with adequate Al contents, nevertheless, high aluminum concentration leads to the coating brittleness and to a strong tendency to crack. Also Cr additions in the coating are still of great importance, because chromium significantly reduces the critical Al content necessary to develop alumina scale (Ref 10, 11).

When the amount of the primary source of Al (i.e., β-NiAl phase) decreases, the bond coat lose its protective properties, due to the formation of some mixed oxide (e.g., NiO, Cr_2O_3, $Ni(Cr, Al)_2O_4$ spinels or others); the very high growth rate of this kind of oxide phases can reduce the TGO adherence and damage the uniformity of the TGO layer. If some yttrium amount is present in the coating chemical composition, the adherence of the oxide scales increases, irrespectively of the alloy composition and the nature of oxide scale formed (Cr_2O_3 or Al_2O_3) (Ref 7, 12–14).

Bond coats can be deposited by means of several techniques such as vacuum plasma spray (VPS), low-pressure plasma spray (LPPS), air plasma spray (APS), high frequency pulse detonation (HFPD) and high velocity oxygen-fuel (HVOF) (Ref 15–20).

In the literature the polished condition of this kind of coatings is often studied (Ref 20, 21), but the as-sprayed or other conditions could be most relevant for the industrial

Alessio Fossati, Martina Di Ferdinando, and **Ugo Bardi**, INSTM—Consorzio Interuniversitario Nazionale per la Scienza e Tecnologia dei Materiali, Via G. Giusti 9, 50121 Firenze, Italy; and **Andrea Scrivani** and **Carlo Giolli**, Turbocoating SpA, V. Mistrali 7, 43040 Rubbiano di Solignano, Parma, Italy. Contact e-mail: alessio.fossati@gmail.com.

production. The surface roughness values of the thermal sprayed samples depends on the spraying technique, on the process parameters and on the granulometry of the sprayed powders. Moreover, after deposition, the manufacturing process may include many other thermal steps such as vacuum or controlled atmosphere annealing and mechanical treatments such as grit blasting or grinding. These operations sensibly modify the surface condition and can affect the coating's performance. For instance, during the industrial production, if an excessively high roughness value of the bond coat is achieved, the surface can be smoothed by means of several methods to the desired roughness values. These industrial kinds of procedure do not take in account the influence of the morphology, composition and microstructure on the service behavior, and the acceptance of the coating quality could be based simply on few simple roughness parameter values without taking into account all the other factors.

Some literature shows that the surface finishing performed after the thermal spraying process can affect the first stages of the oxidation, promoting the formation of a different oxide scale with different performances (Ref 22–27).

The aim of this paper is to study the differences in the oxidation resistance of VPS CoNiCrAlY coatings after different finishing processes; in particular we examined as-sprayed samples as well as the results of treatments based on grinding and on the physical vapour deposition (PVD) of aluminum coatings after grinding.

2. Materials and Methods

CMSX-4 single crystal nickel based superalloy disk samples (φ 25.4*4 mm), were used as substrates (the nominal composition is reported in the Table 1). Before thermal spraying deposition, the substrates were grit blasted using corundum with a grain size of 60-80 mesh, in order to remove surface oxides and to obtain a suitable roughness for coating adhesion.

The nominal composition of the CoNiCrAlY powder is reported in the Table 1.

The VPS process was performed using an F4 gun from Sulzer Metco and using a plasma jet power in the range of 40-50 kW. The systems used Ar and H_2 as plasma gases. Other deposition parameters are typical for industrial VPS applications.

After spraying, the samples were heat treated by means of a vacuum interdiffusion process of 2 h at 1150 °C. The thermally sprayed and vacuum diffused samples were surface finished in three different ways.

Table 1 Nominal chemical composition of the substrate and of the spraying powders

	Ni	Co	Cr	Al	Y	W	Ta	Ti	Mo	Re	Hf
CMSX-4 substrate	61.2	9.5	6.5	5.6	…	6.0	6.5	1.0	0.6	3.0	0.1
CoNiCrAlY powders	32	38.5	21	8	0.5	…	…	…	…	…	…

The first set of samples (hereafter samples A) was maintained with the original surface roughness produced using the VPS process.

A second set of samples (hereafter samples B) were ground by means of an abrasive wheel in order to obtain lower roughness values, as normally performed during industrial smoothening processes.

A third set of samples (hereafter samples C) was obtained by grinding the disc samples, in the same way as for the second set, but, after this pre-treatment, these samples were coated by means of a physical vapour deposition (PVD) process. PVD coatings were produced using an industrial EA-PVD coating apparatus, modified with an Electro Magnetic Controlled Arc Stirring (EMCAS) device. The EMCAS system, as previously described (Ref 28), is an electromagnetic device which can control the electric arc dimension and movement (scanning speed and scanning position) and the correlated parameters such as plasma density and temperature, target wear and evaporation zone. The complete deposition procedure, already used to produce TiO_2 thin coatings, is patented (Ref 29).

For the PVD process, a pure aluminum target was used in an oxygen rich treatment atmosphere in order to produce some aluminum pre-oxidation and allow to the formation of aluminum oxide nuclei. The thickness of the deposited layer was 3.5 ± 0.5 μm.

Isothermal oxidation tests of the three different coated specimen types were conducted at the same time and in the same high temperature furnace at 1000 °C in air, in order to assure identical experimental conditions. Samples were analyzed after 1000, 3000 and 5000 h of test. The cooling down of the samples was carried out inside the furnace reaching about the room temperature in about 24 h. This condition was chosen in order to limit spalling phenomena due to an elevated thermal mismatch between the CoNiCrAlY coating and the thermally grown oxide (TGO) layer. For each kind of sample and oxidation time three specimens were tested. The results related to the oxidized samples were compared with those of the untested ones.

The microstructure and morphology of the coatings were investigated by means of optical microscopy (Nikon Eclipse LV150) and scanning electron microscopy (SEM) (ISI 100B). The chemical composition of the surface was measured by means of EDX microanalysis (NORAN NSS 300). X-ray diffraction analysis (D8 Advance), was performed on the surface of the coatings using the Bragg-Brentano configuration and Cu-Kα radiation, in order to estimate the relative amount of the main surface phases.

The average roughness of the sample surfaces was measured by means of a contact profilometer (Hommel Tester W55). The measures were obtained performing 5 different and independent tests in randomly chosen areas of the samples. The measures were performed scanning 15 mm of surface at 0.2 mm s^{-1} of scan rate. The parameters employed were $\lambda_c = 2.5$ mm and $\lambda_c/\lambda_s = 300$ using a filter ISO 11562(MI); for every type of sample the R_a (arithmetical mean roughness), R_z (average of the 5 maximum heights of the profile) and R_t (maximum distance

between the highest peak and the lowest groove over all the measurement distance) values were calculated.

The thickness of the entire coating, of the interdiffusion layers and of the Al-depleted layers were measured by optical and SEM analysis of the sample cross sections.

Sample cross sections were also utilized in order to study the TGO microstructure and to estimate the chemical composition of the Al-rich and Al-depleted zones by means of EDX microanalysis.

3. Results and Discussion

3.1 Visual Inspection

Figure 1 shows a compound picture that compares the surfaces of the samples before and after different periods of the oxidation test. Before the test, every kind of sample shows a different appearance. The appearance of sample A is typical for one of the as sprayed samples; particularly the roughness has to be noted. The grinding operations performed on samples A produce samples B, smoother and more light reflecting. Nevertheless, if a PVD Al/oxygen coating, is applied on samples B, samples C are produced and their reflecting power is partially lost.

After 1000 h of oxidation test at 1000 °C the surfaces were modified. Samples A show the typical blue color of Co-containing oxides (Ref 30, 31). The color is continuous and homogeneous indicating that no visually detectable spalling occurred. The cases of samples B and C are different. Both kinds of samples show a non homogeneous coloration; particularly the blue color is the minor color, whereas the grey color is the dominant one. The non homogeneous color could be ascribed to a general production of alumina (a thin alumina layer is quite transparent and allows the metallic coating interface to reflect the visible light (Ref 32–34)) and to the localized presence of Co-containing scale (blue color). Local mixed oxide formation could be due to several reasons such as: (1) preoxidized cavities present between the different splats (in the case of sample B), (2) cobalt diffusion through the aluminum deposited layer (in the case of sample C) or 3) spalling phenomena.

Even after 5000 h of oxidation test at 1000 °C the sample surface condition appears relatively stable. Nevertheless some changes can be observed; in the case of

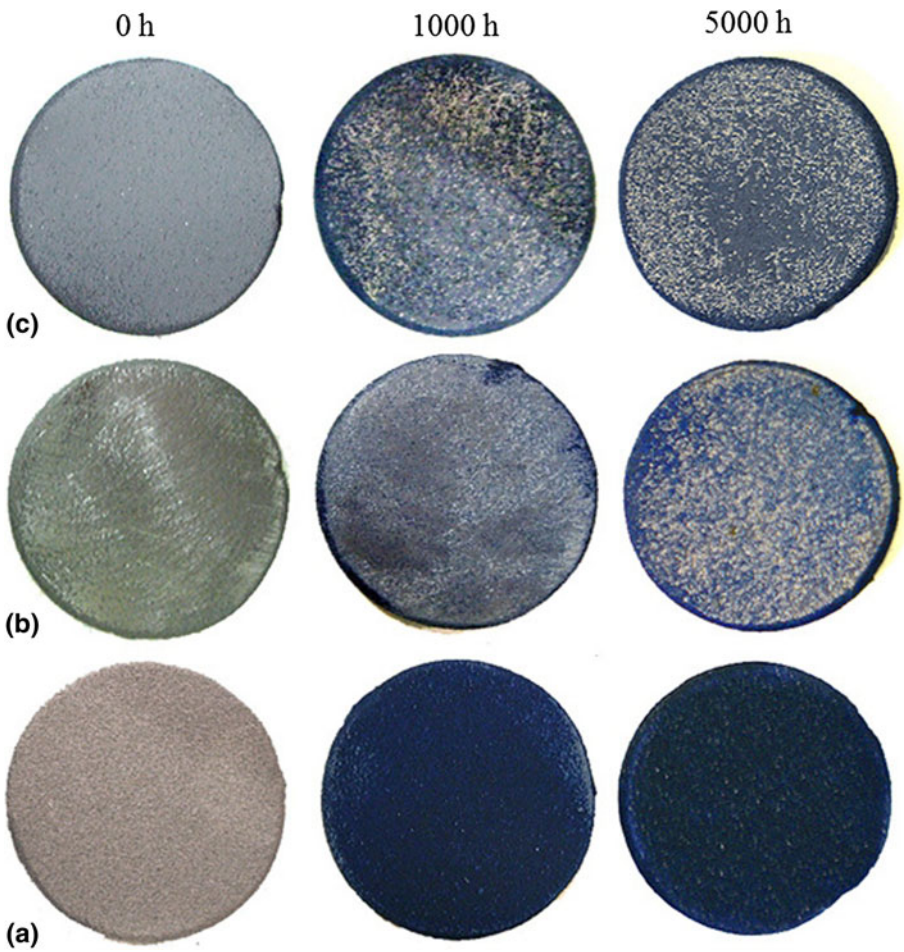

Fig. 1 The picture shows samples A-C before and after different periods of isothermal oxidation in air at 1000 °C. (Color figure online)

samples A the blue color is changing toward a grey, whereas samples B tend to form some more blue-colored oxide. The behavior of the two kinds of samples could be explained as follows. Samples A tend to replace Co-containing oxide with more adherent alumina, whereas samples B tend to form Co-containing oxide due to the depletion of the aluminum reservoir.

3.2 X-Ray Diffraction Analysis

Figure 2 shows the XRD patterns of untested samples; spectra appear different each other. The analysis performed onto the untreated samples A showed the presence of both γ-(Co,Ni) and β-(Co,Ni)Al phases where the latter phase is the predominant one; moreover the diffraction peaks of this kind of samples are sharp, suggesting a relatively large crystallite dimension.

In the case of samples B, the same phases are detected and the β-(Co,Ni)Al phase remains the predominant one, but its relative amount decrease in comparison with that of samples A; moreover, the diffraction peaks of both the phases appear sensibly broadened indicating a smaller crystallite grain size in respect of that of samples A. The smaller crystallite size could be ascribed to the presence of a plastically deformed thin tribological layer produced by the grinding process performed by hand by using an abrasive wheel. As already known in the literature a severe plastic deformation of the surface grains produces the decrease of their crystallite size (Ref 35–37).

In the case of sample C, the pattern shows the presence of sharp aluminum peaks and broadened γ-(Co,Ni) peaks; β-(Co,Ni)Al peaks are not clearly detectable due to the overlap with the stronger aluminum peaks. In the case of samples C it has to be noted that diffraction peaks of aluminum oxide are not detectable; this result cannot exclude the presence of a very thin aluminum oxide layer or some aluminum oxide nuclei not detectable by the XRD measurements, instead it could be confirm the little dimension of this oxide layer. In fact, the high affinity of the aluminum toward the oxygen, which is present in the treatment atmosphere utilized during the PVD process, should provide some kind of reaction between these two chemical elements.

In Fig. 3 the XRD patterns of tested samples after 1000 h of the oxidation test at 1000 °C are reported. Oxidized sample patterns are different in comparison with those of the untested samples. The patterns of samples B and C are similar, differing from those of the oxidized A samples. Samples A show a surface that is composed of comparable amounts of α-alumina and $(Co,Ni)(Cr,Al)_2O_4$ spinel, in agreement with the visual inspection that observed the presence of blue colored oxide. In contrast, samples B and C show a surface essentially composed of α-alumina, in agreement with the observed surface grey color. Moreover, $(Co,Ni)(Cr,Al)_2O_4$ spinel oxide peaks and some peak (at 33.3° there is the strongest one) that could be ascribed to $Y_3Al_5O_{12}$ were detected on the surface, the estimated amount of the latter phase is very low and was not reported in the figure. Metallic aluminum peaks are no more detectable on the surface of samples C indicating that a sufficiently thick α-alumina layer was formed and/or the aluminum diffused into the CoNiCrAlY coating.

Even after 5000 h of test, the XRD patterns maintain the main features of those collected after 1000 h, in agreement with the visual inspection observation. In the end, no Cr_2O_3 peaks were detected on any kind of sample, according to the presence of the aluminum reservoir well observed in the cross sections, even after 5000 h of test (Fig. 4).

For the sake of completeness we report that XRD analysis performed on samples A-C just after 2 h of oxidation at 1000 °C shows the same qualitative results obtained for longer exposition; samples A presents TGO layers formed by both α-alumina and $(Co,Ni)(Cr,Al)_2O_4$ spinel oxide, while samples B and C show TGO layers essentially

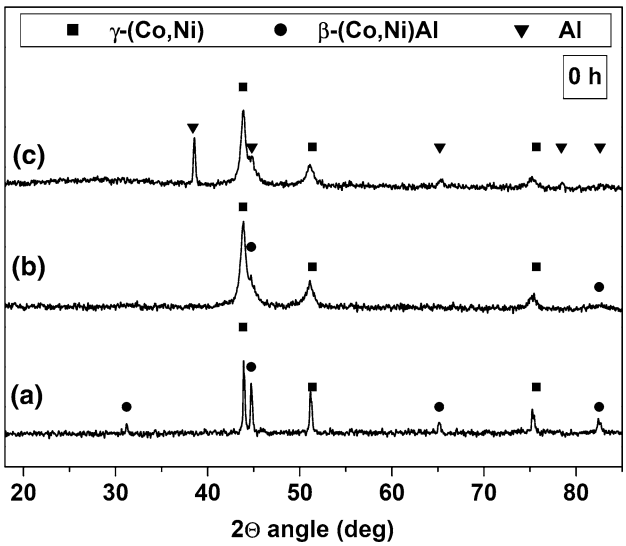

Fig. 2 XRD patterns of the surface of samples A-C before the oxidation test

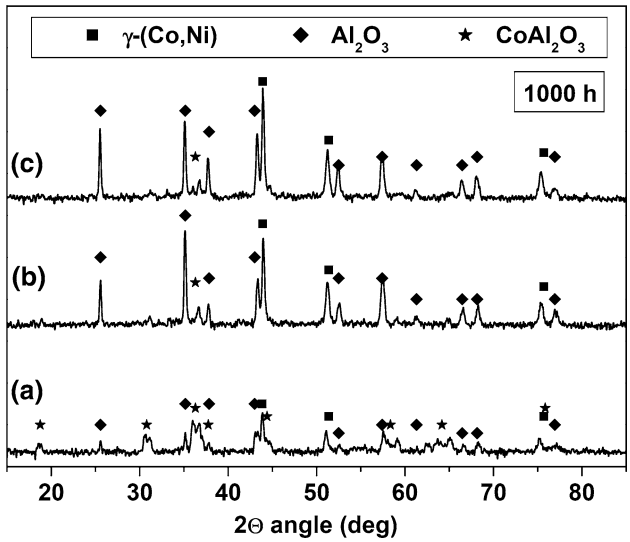

Fig. 3 XRD patterns of the surface of samples A-C after 1000 h of isothermal oxidation at 1000 °C

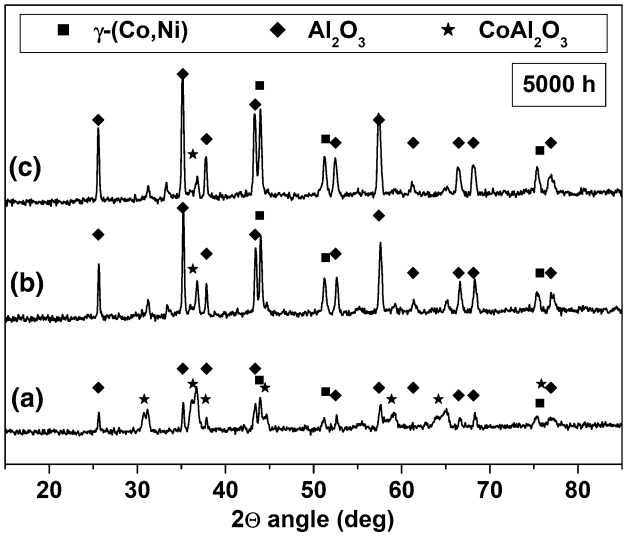

Fig. 4 XRD patterns of the surface of samples A-C after 5000 h of isothermal oxidation at 1000 °C

composed by α-alumina (no transitional γ-alumina diffraction peak could be revealed in any kind of samples). This result is in agreement with a similar study performed using other kind of CoNiCrAlY bond coats (Ref 38).

3.3 Surface Composition

In Fig. 5 the surface composition of samples A-C before and after different oxidation periods are reported. Surface compositions are in good agreement with x-ray analysis and visual inspection. In the case of samples A the initial aluminum surface concentration indicates only a modest degree of preferential oxidation, which probably occurred during the low vacuum high temperature interdiffusion treatment. Nevertheless the observed amount of aluminum is not high enough to be detectable as oxide layer by x-ray diffraction. During the test, the surface aluminum concentration increases whereas the cobalt concentration decreases, in agreement with the trend of the quite homogeneous loss of the blue color, due to the α-alumina amount increase.

Surface analyses performed on samples B indicate that the grinding operations are able to remove essentially all the oxides potentially formed during the first stages of the production. This leads to surface concentrations comparable with those of the nominal powder concentration values. After the first 1000 h of the oxidation test, the surface composition reveals the preferential formation of aluminum and yttrium containing oxides, as observed by other authors (Ref 39–41). This result is in agreement with the x-ray diffraction analysis that showed the prevalence of the Al_2O_3 and to the visual inspection that did not observed a complete blue colored oxide coverage of the samples. As the oxidation test proceeds, Cr, Co and Ni concentrations increase, whereas Al and Y concentrations decrease; suggesting the decrease of the concentration of Al_2O_3 and the increase of the quantity of the other oxide types.

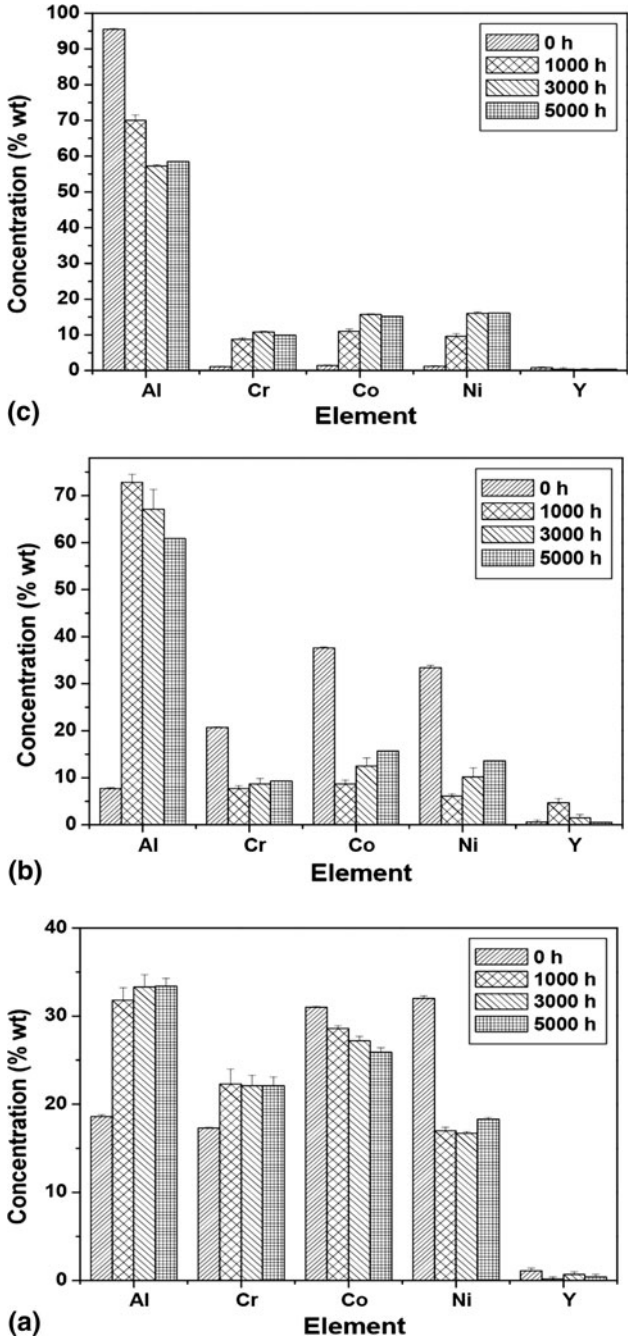

Fig. 5 Surface composition of samples A-C before and after different periods of isothermal in air at 1000 °C

Before the test, the surface of samples C contains essentially aluminum suggesting a good coverage of the PVD layer. The low concentrations of Cr, Co and Ni observed can be ascribed to the x-ray signal collected from the deeper bond coat layers. During the test, the Al surface concentration decreases while Co, Cr and Ni concentrations increase. The elemental concentrations after 3000 and 5000 h of test are comparable. This is in agreement with the surface stability observed by visual inspection and x-ray diffraction analysis. Moreover, no yttrium

surface concentration sharp increase can be detected after the first 1000 h of oxidation, because the PVD layer does not contain this element.

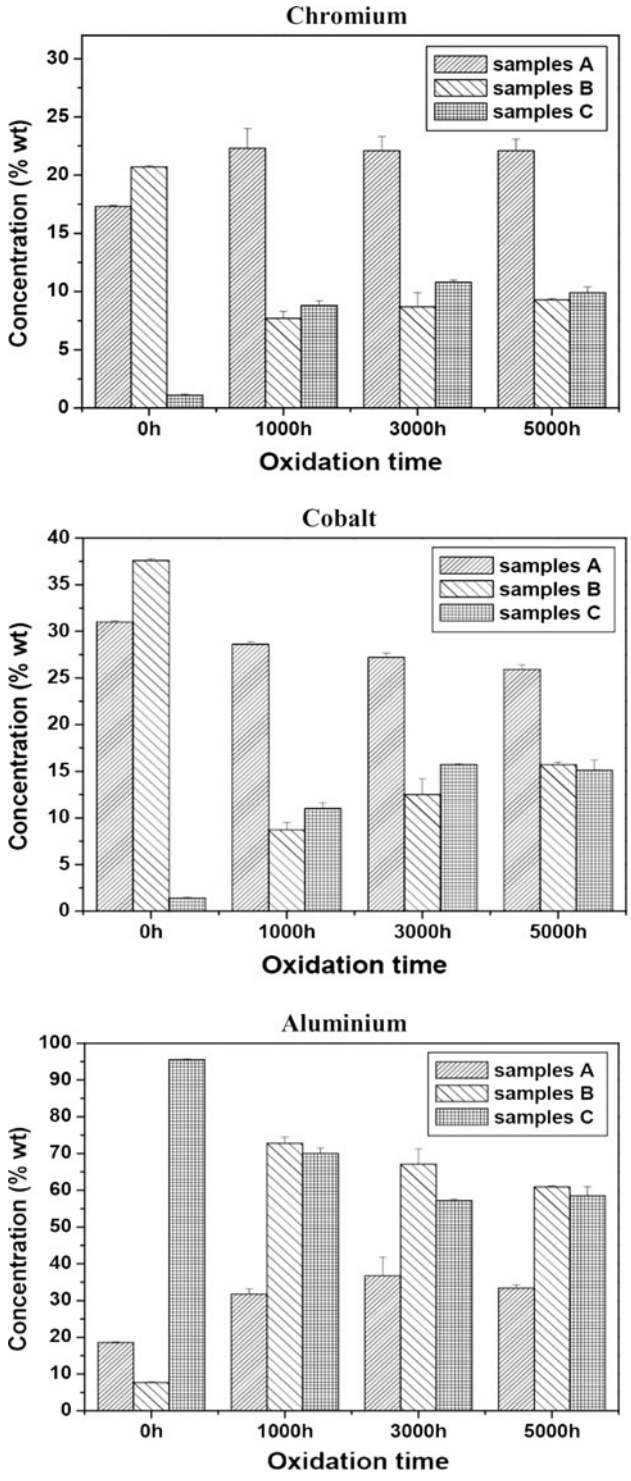

Fig. 6 Chromium, cobalt and aluminum surface concentration of the different kinds of samples after various oxidation periods at 1000 °C

Figure 6 shows a comparison of the surface concentrations of the most important oxide-forming elements (Al, Cr and Co).

In the case of chromium, note that this element has an approximately stable concentration for every kind of samples, except for the ''as sprayed'' ones. Samples A have a Cr concentration that is higher in comparison with B and C samples confirming the stability of the Cr-containing oxide formed during the first stages of the oxidation and the practical absence of spalling phenomena.

In the case of cobalt, clear concentration trends can be observed. In particular, samples A show a decrease of cobalt concentration, while samples B and C constantly show an increase.

Samples A show a good stability of aluminum concentration after 1000 h of treatment. Conversely, the aluminum concentration decreases on samples B and C. Nevertheless, the absolute surface concentration values detected on samples B and C are always higher in comparison with those of samples A. This is in agreement with x-ray diffraction analysis that observed the prevalent presence of α-alumina onto the surfaces of samples B and C.

3.4 Roughness Measurements

Table 2 reports the average roughness parameter values, measured for each kind of sample and for every oxidation period.

In the case of samples A, the roughness parameter evolution with time suggests a good surface morphology stability, in agreement with the very little delamination phenomena observed.

In the case of samples B the grinding operations sensibly lower the roughness values—a condition maintained during the first 1000 h of oxidation. Samples oxidized for a period equal or longer than 3000 h show a sensible increase of the roughness. This result could be ascribed to the starting of some delamination or to oxidation phenomena, presumably due to the lower protection ability of the TGO surface layers formed on ground surfaces.

In the case of samples C it can be observed that the PVD coating process is able to further reduce the roughness values in comparison with those of the samples B.

Table 2 Surface roughness parameters of the various kinds of samples before and after different periods of isothermal oxidation in air at 1000 °C

	0 h	1000 h	3000 h	5000 h
R_a				
A	17.3 ± 1.0	17.0 ± 0.7	16.7 ± 1.2	17.2 ± 1.1
B	6.1 ± 1.1	6.1 ± 1.2	10.0 ± 0.5	11.0 ± 0.8
C	4.3 ± 0.4	4.6 ± 0.5	5.1 ± 0.4	4.7 ± 0.3
R_z				
A	101.0 ± 6.5	104.1 ± 6.9	101.5 ± 8.2	102.6 ± 8.4
B	45.8 ± 6.3	45.1 ± 4.6	62.0 ± 3.0	68.5 ± 4.6
C	38.6 ± 4.5	37.2 ± 4.1	38.5 ± 2.9	38.7 ± 2.5
R_t				
A	124.4 ± 13.9	126.1 ± 11.5	123.9 ± 6.3	124.4 ± 13.6
B	56.3 ± 5.6	57.5 ± 7.7	77.3 ± 7.7	88.0 ± 9.9
C	53.5 ± 8.9	48.3 ± 1.5	51.9 ± 7.6	52.7 ± 1.3

During the oxidation tests no significant changes of the roughness parameters values were detected. This behavior could be correlated to the enhancement of the oxidation resistance due to the PVD coating which seems to be able to delay corrosion phenomena when applied onto a ground surface that by itself would not be able to form a very protective scale. The surface morphology analysis (reported separately) suggests the presence of delamination phenomena, but the surface appears stable.

3.5 Surface Morphology

In Fig. 7 we show the results obtained by means of electron microscopy regarding to the morphology of the different kind of samples before and after various periods of oxidation at 1000 °C.

In the case of samples A the surface appears very rough, due to the presence of splats and unmelted powder particles. As the oxidation time increases, nucleation and growth of the oxide scale becomes more and more relevant, as shown by the sample charging under the electron beam; moreover, no significant delamination zones were detected, in agreement with the visual inspection and with the EDX analysis.

In the case of samples B, the untreated specimens show the typical morphology of coarsely ground surfaces. The grinding operations did not remove a very large thickness of material, but the shape of the splatted powders is still visible, appearing as dishomogeneities and cavities. The non homogeneous blue coloration of this kind of samples could be ascribed to the oxidation of these zones that have the same surface characteristics of those of the samples A. Only after 3000 h of test spalling phenomena become relevant and well detectable by SEM. In Fig. 8 a detail of the surface of one of the B type samples after 3000 h of test it is shown. Spallation phenomena lead to the appearance of the unoxidized coating surface; the mixed oxides (clearer zones in the SEM micrograph) grow onto aluminum based oxides (darker regions).

In the case of the untested samples C the PVD coating fills and partially closes the cavities, producing the surface leveling observed by roughness measurements. After 1000 h of the oxidation test at 1000 °C the first spalling events can be detected. However, the surface roughness remains stable and no relevant corrosion cavities were detected even after 5000 h.

3.6 Cross Sections and Al-Depleted Zones

Some typical optical microscopy cross section micrographs, obtained before and after different oxidation periods of time for each kind of sample, are reported in Fig. 9.

The bond coat thickness for each type of sample was about 300 μm. The as-coated samples showed the presence of both the γ-(Co,Ni) and β-(Co,Ni)Al phases across the entire thickness. A very thin interdiffusion layer (<10 μm) was detected between the bond coat and the superalloy substrate, due to the initial low vacuum high temperature heat treatment. The interdiffusion layer is thinner in

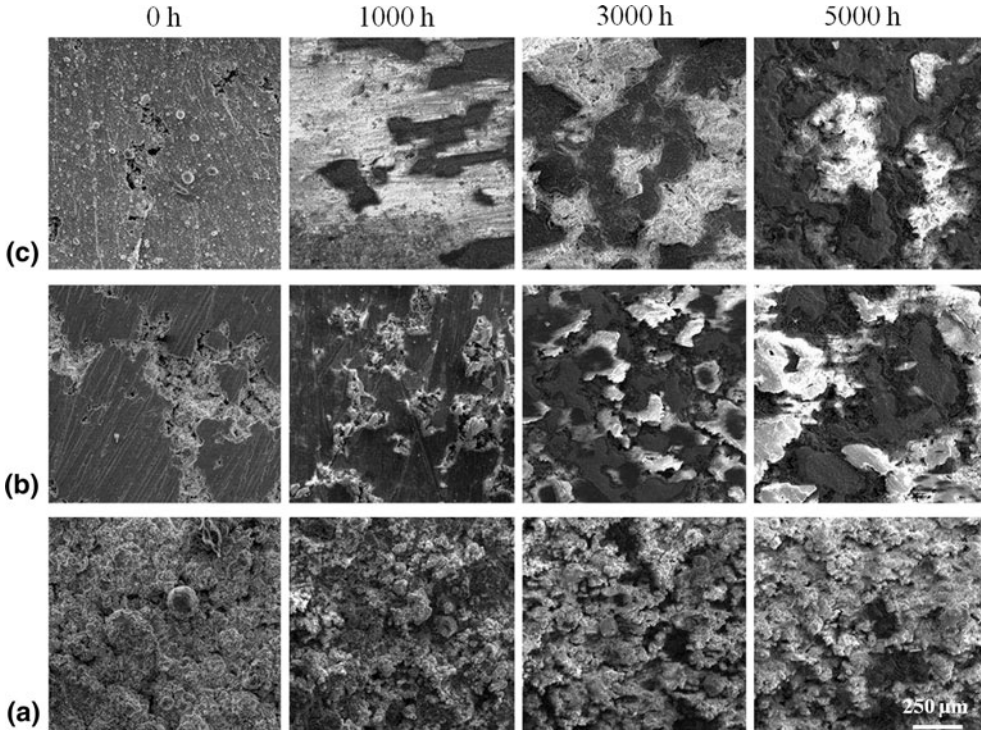

Fig. 7 SEM micrographs showing the morphology evolution of the surface of samples A-C before and after different periods of isothermal oxidation at 1000 °C

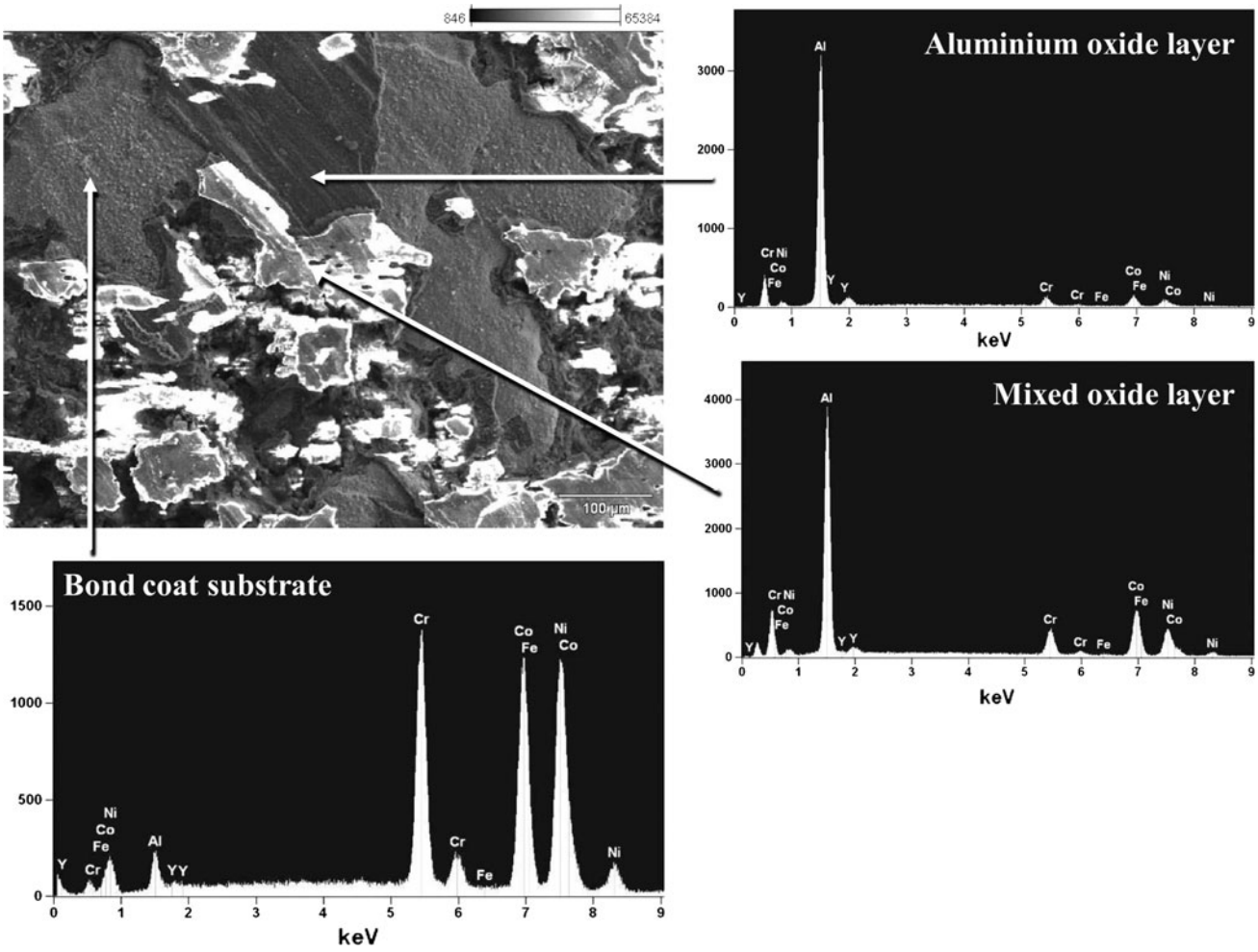

Fig. 8 SEM micrograph and spot EDX spectra of a sample B after 3000 h of exposition. The arrows indicate the different regions where microanalysis has been performed

comparison with those detected for coatings sprayed onto polycrystalline superalloys and subject to the same vacuum interdiffusion process (Ref 19, 42), probably due to the lower diffusion coefficient in the case of a single crystal alloy.

During the high temperature oxidation tests, the aluminum diffusion toward the coating surface to form the TGO layer produces an external Al-depletion zone. No internal Al-depletion layer was detected, as it has been observed in our previous work in the case of polycrystalline substrates (Ref 19, 20, 42). The external Al-depletion zone thickness increases during the tests. This augment of thickness and thus of the expected life of the coatings are different, depending on the surface finishing treatment.

For all the types of samples analyses performed in the Al-reservoir zones showed that Ni, Ta and W concentrations increased during the oxidation, whereas Co and Cr content decreased.

Samples A and samples C showed a higher oxidation resistance in comparison with samples B. The main difference of samples A and B concerns not only the surface roughness but the removal of the external pre-oxidized layers. In the literature many articles report that lower roughness values can improve the oxidation resistance (Ref 24, 25, 43, 44), but most of the reported results are relative to samples that were ground, even if in different way, without any comparison with as-deposited surfaces. In our experiment, in which we compared as-sprayed samples versus ground ones, the surface of samples A maintained the same surface phases formed during the spraying process (and/or during the low vacuum interdiffusion process), whereas in the case of samples B these surface oxides were removed. The different oxidation resistance suggests that some oxide nuclei that presumably form during the spraying process and/or the low vacuum interdiffusion treatment play a very important role in controlling the protection abilities of the TGO layer. It seems that the first oxide nuclei or the very thin oxide layers formed during the high temperature spraying process and/or the high temperature low vacuum interdiffusion processes allow the growth of more protective TGO layers.

The Al reservoir of the samples C appears to be less depleted in comparison with that of samples B. This can suggest that the PVD coating leads to the formation of a

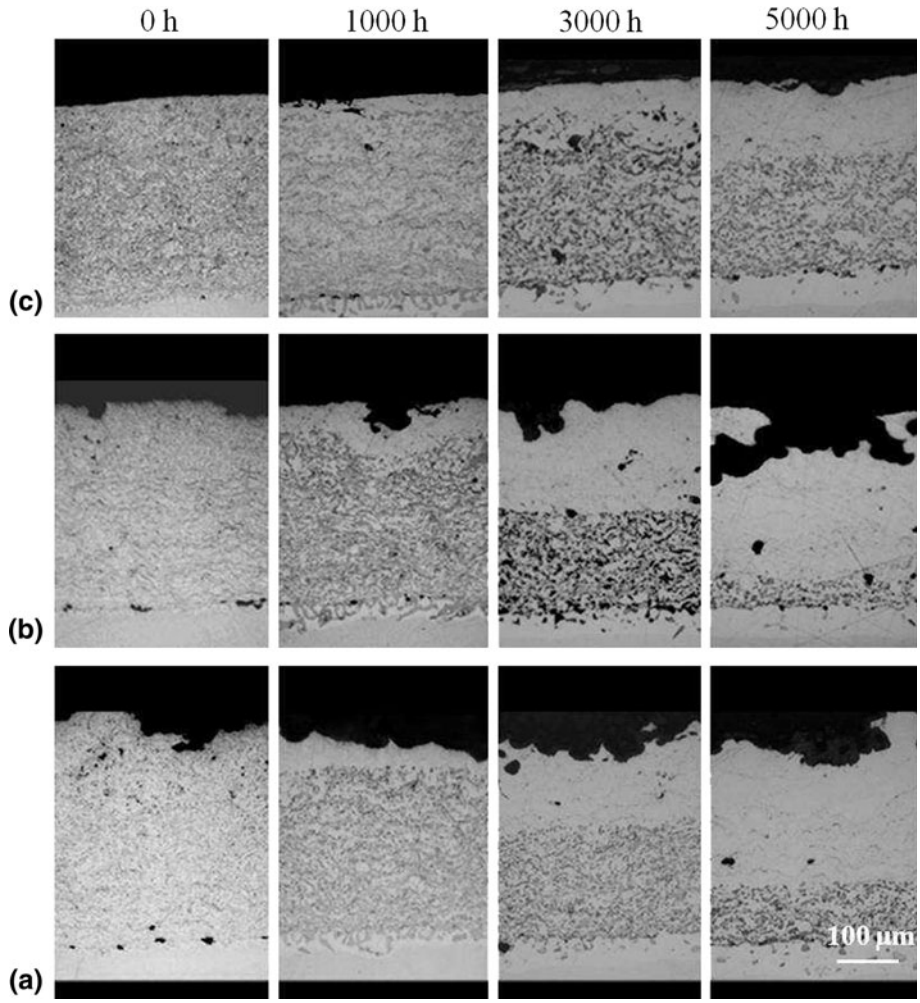

Fig. 9 Optical micrographs of the cross sections of the samples A-C before and after different periods of isothermal oxidation at 1000 °C

more protective TGO layer even when the surface layers were removed by grinding operations. Because the PVD process is performed by means of an aluminum target in oxygen atmosphere, it can be hypothesized that this treatment leads to the formation of oxide nuclei or oxide thin layers that help the growth of a highly protective TGO layer.

Comparing the oxidation resistance of samples A-C, it appears that the PVD Al/oxygen coatings can provide significant benefits. First of all, these coatings can solve the problem of the reduction of the oxidation resistance due to the removal by grinding of the first surface pre-oxidized layers. Furthermore, the PVD coating enhances the oxidation resistance of ground samples up to a level higher than the as-sprayed samples. This suggests to perform PVD Al/oxygen treatment as pre-treatment in the case of the deposition of YPSZ top coat obtained by EB-PVD.

4. Conclusions

In this paper the isothermal high temperature oxidation behavior of CoNiCrAlY coatings of comparable thickness produced by VPS onto CMSX-4 single crystal nickel superalloy substrates has been studied. Three kinds of samples with different surface finishing procedures were considered: as-sprayed, ground and PVD coated after grinding. After spraying, all the samples were annealed at high temperatures in low vacuum. The PVD process consisted of aluminum deposition in oxygen rich atmosphere.

Morphological, microstructural and compositional analyses were performed in order to produce a complete characterization of the samples before and after the oxidation tests carried out at 1000 °C up to 5000 h.

The three types of samples showed considerable differences in their behavior. As-sprayed samples and PVD coated samples showed an oxidation resistance higher than ground samples; in particular PVD coated samples presented the highest expected life. The grinding operation decreases the oxidation resistance; this seems to be ascribable to the removal of the oxide nuclei formed during the thermal spraying process and/or during the low vacuum annealing treatment. The presence of this kind of nuclei promote the formation of a higher quality oxide scale with better protection performances. The use of the

PVD of aluminum, in oxygen atmosphere, promote the production of a very protective scale even onto pre-ground samples. This kind of PVD process could be used when grinding operations were performed in order to achieve the right roughness to deposit a ceramic top coat without loosing the oxidation resistance properties of the as-sprayed and pre-oxidized surfaces; moreover, this finishing process could be able to produce high temperature resistant and smooth components.

Acknowledgment

This work was supported by the FIRB Project No. RBIP06X7F4.

References

1. N.P. Padture, M. Gell, and E.H. Jordan, Thermal Barrier Coatings for Gas-Turbine Engine Applications, *Science*, 2002, **296**, p 280-284
2. J.R. Nicholls, N.J. Simms, W.Y. Chan, and H.E. Evans, Smart Overlay Coatings—Concept and Practice, *Surf. Coat. Technol.*, 2002, **149**(2-3), p 236-244
3. P.K. Wright and A.G. Evans, Mechanisms Governing the Performance of Thermal Barrier Coatings, *Curr. Opin. Solid State Mater. Sci.*, 1999, **4**(3), p 255-265
4. A. Atkinson, A. Selcuk, and S.J. Webb, Variability of Stress in Alumina Corrosion Layers Formed in Thermal-Barrier Coatings, *Oxid. Met.*, 2000, **54**(5-6), p 371-384
5. B.A. Pint, I.G. Wright, W.Y. Lee, Y. Zhang, K. Prüßner, and K.B. Alexander, Substrate and Bond Coat Compositions: Factors Affecting Alumina Scale Adhesion, *Mater. Sci. Eng. A.*, 1998, **245**(2), p 201-211
6. A.G. Evans, D.R. Mumm, J.W. Hutchinson, G.H. Meier, and F.S. Pettit, Mechanis, Controlling, the Durability of Thermal Barrier Coatings, *Prog. Mater. Sci.*, 2001, **46**(5), p 505-553
7. A.G. Evans, D.R. Clarke, and C.G. Levi, The Influence of Oxides on the Performance of Advanced Gas Turbines, *J. Eur. Ceram. Soc.*, 2008, **28**, p 1405-1419
8. P.Y. Hou, Impurity Effects on Alumina Scale Growth, *J. Am. Ceram. Soc.*, 2003, **86**, p 660-668
9. K. Messaoudi, A.M. Huntz, and B. Lesage, Diffusion and Growth Mechanism Of Al_2O_3 Scales on Ferritic Fe-Cr-Al Alloys, *Mater. Sci. Eng. A*, 1998, **247**(1-2), p 248-262
10. E.A.G. Shillington and D.R. Clarke, Spalling Failure of a Thermal Barrier Coating Associated with Aluminum Depletion in the Bond-Coat, *Acta Mater.*, 1999, **47**, p 1297-1305
11. W. Brandl, H.J. Grabke, D. Toma, and J. Krüger, The Oxidation Behaviour of Sprayed MCrAlY coatings, *Surf. Coat. Technol.*, 1996, **86-87**, p 41-47
12. L. Ajdelsztajn, F. Tang, G.E. Kim, V. Provenzano, and J.M. Schoenung, Synthesis and Oxidation Behavior of Nanocrystalline MCrAlY Bond Coatings, *J. Therm. Spray Technol.*, 2005, **14**, p 23-30
13. A. Rabiei and A.G. Evans, Failure Mechanisms Associated with the Thermally Grown Oxide in Plasma-Sprayed Thermal Barrier Coating, *Acta Mater.*, 2000, **48**(15), p 3963-3976
14. J.L. Smialek, D.T. Jayne, J.C. Schaffer, and W.H. Murphy, Effects of Hydrogen Annealing, Sulfur Segregation and Diffusion on the Cyclic Oxidation Resistance of Superalloys: A Review, *Thin Solid Films*, 1994, **253**(1-2), p 285-292
15. J.A. Haynes, M.K. Ferber, and W.D. Porter, Thermal Cycling Behavior of Plasma-Sprayed Thermal Barrier Coatings with Various Mcraix Bond Coats, *J. Therm. Spray Technol.*, 2000, **9**(1), p 38-48
16. A. Peichl, T. Beck, and O. Vöhringer, Behaviour of an EB-PVD Thermal Barrier Coating System Under Thermal-Mechanical Fatigue Loading, *Surf. Coat. Technol.*, 2003, **162**(2-3), p 113-118
17. F.J. Belzunce, V. Higuera, and S. Poveda, High Temperature Oxidation of HFPD Thermal-Sprayed MCrAlY Coatings, *Mater. Sci. Eng. A*, 2001, **297**(1-2), p 162-167
18. Kh.G. Schmitt-Thomas, H. Haindl, and D. Fu, Modifications of Thermal Barrier Coatings (TBCS), *Surf. Coat. Technol.*, 1997, **94-95**, p 149-154
19. M. Di Ferdinando, A. Fossati, A. Lavacchi, U. Bardi, F. Borgioli, C. Borri, C. Giolli, and A. Scrivani, Isothermal Oxidation Resistance Comparison Between Air Plasma Sprayed, Vacuum Plasma Sprayed and High Velocity Oxygen Fuel Sprayed Conicraly Bond Coats, *Surf. Coat. Technol.*, 2010, **204**(15), p 2499-2503
20. A. Fossati, M. Di Ferdinando, A. Lavacchi, U. Bardi, C. Giolli, and A. Scrivani, Improvement of the Isothermal Oxidation Resistance of Conicraly Coating Sprayed by High Velocity Oxygen Fuel, *Surf. Coat. Technol.*, 2010, **204**(21–22), p 3723-3728
21. H. Choi, B. Yoon, H. Kim, and C. Lee, Isothermal Oxidation of Air Plasma Spray Nicraly Bond Coatings, *Surf. Coat. Technol.*, 2002, **150**(2-3), p 297-308
22. D. Toma, W. Brandl, and U. Köster, Studies on the Transient Stage of Oxidation of VPS and HVOF Sprayed Mcraly Coatings, *Surf. Coat. Technol.*, 1999, **120-121**, p 8-15
23. A. Gil, V. Shemet, R. Vassen, M. Subanovic, J. Toscano, D. Naumenko, L. Singheiser, and W.J. Quadakkers, Effect of Surface Condition on the Oxidation Behaviour of Mcraly Coatings, *Surf. Coat. Technol.*, 2006, **201**(7), p 3824-3828
24. D. Zhang, S. Gong, H. Xu, and Z. Wu, Effect of Bond Coat Surface Roughness on the Thermal Cyclic Behavior of Thermal Barrier Coatings, *Surf. Coat. Technol.*, 2006, **201**(3-4), p 649-653
25. N. Czech, M. Juez-Lorenzo, V. Kolarik, and W. Stamm, Influence of the Surface Roughness on the Oxide Scale Formation on Mcraly Coatings Studied In Situ by High Temperature X-Ray Diffraction, *Surf. Coat. Technol.*, 1998, **108-109**, p 36-42
26. L. Xie, Y. Sohn, E.H. Jordan, and Maurice. Gell, The Effect of Bond Coat Grit Blasting on the Durability and Thermally Grown Oxide Stress in an Electron Beam Physical Vapor Deposited Thermal Barrier Coating, *Surf. Coat. Technol.*, 2003, **176**(1), p 57-66
27. M.-J. Pindera, J. Aboudi, and S.M. Arnold, The Effect of Interface Roughness and Oxide Film Thickness on the Inelastic Response of Thermal Barrier Coatings to Thermal Cycling, *Mater. Sci. Eng. A*, 2000, **284**(1-2), p 158-175
28. C. Giolli, F. Borgioli, A. Credi, A. Di Fabio, A. Fossati, M. Muniz Miranda, S. Parmeggiani, G. Rizzi, A. Scrivani, S. Troglio, A. Tolstoguzov, A. Zoppi, and U. Bardi, Characterization of TiO_2 Coatings Prepared by a Modified Electric Arc-Physical Vapour Deposition System, *Surf. Coat. Technol.*, 2007, **202**(1), p 13-22
29. European Patent Application EP 1 624 087 A1
30. M. Lusar, A. Forés, J.A. Badenes, J. Calbo, M.A. Tena, and G. Monrós, Colour Analysis of Some Cobalt-Based Blue Pigments, *J. Eur. Ceram. Soc.*, 2001, **21**, p 1121-1130
31. W. Li, J. Li, and J. Guo, Synthesis and Characterization of Nanocrystalline $CoAl_2O_4$ Spinel Powder by Low Temperature Combustion, *J. Eur. Ceram. Soc.*, 2003, **23**, p 2289-2295
32. J. Petit, P. Dethare, A. Sergent, R. Marino, M.-H. Ritti, S. Landais, J.-L. Lunel, and S. Trombert, Sintering of α-Alumina for Highly Transparent Ceramic Applications, *J. Eur. Ceram. Soc.*, 2011, **31**, p 1957-1963
33. B.-N. Kim, K. Hiraga, K. Morita, and H. Yoshida, Effects of Heating Rate on Microstructure and Transparency of Spark-Plasma-Sintered Alumina, *J. Eur. Ceram. Soc.*, 2009, **29**, p 323-327
34. T.I. Selinder, E. Coronel, E. Wallin, and U. Helmersson, α-Alumina Coatings on WC/Co Substrates by Physical Vapor Deposition, *Int. J. Refract Met. H.*, 2009, **27**, p 507-512
35. R.Z. Valiev, R.K. Islamgaliev, and I.V. Alexandrov, Bulk Nanostructured Materials From Severe Plastic Deformation, *Prog. Mater. Sci.*, 2000, **45**, p 103-189
36. W. Österle and P.X. Li, Mechanical and Thermal Response of a Nickel-Base Superalloy Upon Grinding with High Removal Rates, *Mater. Sci. Eng. A*, 1997, **238**, p 357-366
37. K. Lu and J. Lu, Nanostructured Surface Layer on Metallic Materials Induced by Surface Mechanical Attrition Treatment, *Mater. Sci. Eng. A*, 2004, **375-377**, p 38-45

38. F. Tang, L. Ajdelsztajn, G.E. Kim, V. Provenzano, and J.M. Schoenung, Effects of Surface Oxidation During HVOF Processing on the Primary Stage Oxidation of a CoNiCrAlY Coating, *Surf. Coat. Technol.*, 2004, **185**(2-3), p 228-233
39. A. Gil, D. Naumenko, R. Vassen, J. Toscano, M. Subanovic, L. Singheiser, and W.J. Quadakkers, Y-Rich Oxide Distribution in Plasma Sprayed MCrAlY-Coatings Studied by SEM with a Cathodoluminescence Detector and Raman Spectroscopy, *Surf. Coat. Technol.*, 2009, **204**(4), p 531-538
40. R. Cueff, H. Buscail, E. Caudron, C. Issartel, and F. Riffard, Oxidation of Alumina Formers at 1173 K: Effect of Yttrium Ion Implantation and Yttrium Alloying Addition, *Corr. Sci.*, 2003, **45**(8), p 1815-1831
41. P. Castello, F.H. Stott, and F. Gesmundo, Yttrium-Promoted Selective Oxidation of Aluminium in the Oxidation At 1100°C of an Eutectic Ni-Al-Cr_3C_2 Alloy, *Corr. Sci.*, 1999, **41**(5), p 901-918
42. A. Fossati, M. Di Ferdinando, A. Lavacchi, A. Scrivani, C. Giolli, and U. Bardi, Improvement of the Oxidation Resistance of CoNiCrAlY Bond Coats Sprayed by High Velocity Oxygen-Fuel onto Nickel Superalloy Substrate, *Coatings*, 2011, **1**, p 3-16
43. G. Lee, A. Atkinson, and A. Selçuk, Development of Residual Stress and Damage in Thermal Barrier Coatings, *Surf. Coat. Technol.*, 2006, **201**(7), p 3931-3936
44. M.P. Taylor and H.E. Evans, The Influence of Bond Coat Surface Roughness and Structure on the Oxidation of a Thermal Barrier Coating System, *Mat. Sci. Forum*, 2001, **711**, p 369-372